Measurements of Thermal Ion Drift Velocity and Temperature Using Planar Sensors

R. A. Heelis and W. B. Hanson[1]

William B. Hanson Center for Space Sciences, University of Texas at Dallas, Richardson, 75080

Abstract. Satellite measurements of the ion temperature, velocity, and concentration may be obtained by measuring incident variations in the ion flux using a retarding potential analyzer (RPA). A retarding voltage inside the sensor can be used to control the energy of ions having access to the detector. By examining the variations in this flux as a function of energy, the temperature can be determine. The thermal velocity of low energy ions is frequently much less than satellite orbital velocities, in which case the direction of arrival of the ions is approximately aligned along the satellite velocity vector and does not change greatly. In this case the precise arrival angle of the ions can be obtained by a device called an ion drift meter (IDM), which measures the current asymmetry on a detector surface caused by deviations of the ion beam from normal incidence. There is a simple trigonometrical relationship between the ion arrival angles, the normally incident ion velocity, and the transverse velocity. Here we describe the operating principles embedded in the required measurements and the limitations that are inherent in the various measurement techniques. In the presence of a magnetic field where the ion gyrofrequency exceeds the ion-neutral collision frequency, the ion velocity perpendicular to the magnetic field can be derived from a measurement of the electric field vector and knowledge of the magnetic field vector. These conditions apply in the Earth's ionosphere above about 250 km altitude and the relative merits of electric field and ion drift measurements are discussed for this case.

INTRODUCTION

The thermal ion drift in planetary atmospheres may be directly derived by in-situ sensors on orbiting vehicles measuring the arrival angle of the plasma with respect to some reference direction and the kinetic energy of the plasma along that reference direction. Here we describe the techniques employed by planar sensors when the sensor platform is moving supersonically with respect to the plasma.

Two sensors are employed to derive the ion drift velocity. A planar retarding potential analyzer (RPA) is utilized to measure the energy distribution of the plasma along the sensor look direction. A planar ion drift meter (IDM) is utilized to measure the arrival angle of the plasma with respect to the RPA sensor look direction. Here we will describe the techniques employed in the operation of the sensors and the manner in which prevailing ionospheric conditions may affect the integrity of the measurement. Finally we will briefly discuss factors to be taken into account when a comparison is made between ion velocity measurements and electric field measurements in an environment where the two should be related by the expression $\mathbf{E} = -\mathbf{V}\times\mathbf{B}$.

[1]Deceased

Measurement Techniques in Space Plasmas: Particles
Geophysical Monograph 102

PLANAR RETARDING POTENTIAL ANALYZER

A retarding potential analyzer is a rather generic name used to describe many devices that utilize a retarding potential to control the energy of charged particles that have access to a detector. If the energy distribution of the particles is assumed to be a Maxwellian, then the variation in the particle flux as a function of energy can be used to derive the temperature and the kinetic energy with respect to the sensor of the charged species. Additionally if the sensor has a limited acceptance angle then the kinetic energy along the sensor look direction may be used to derive the charged species velocity along the look direction.

At this point it is helpful to recall that in the atmospheres of Earth, and Venus the velocity of a vehicle in orbit in the ionosphere is about 7.8 km s^{-1}. This velocity imparts an energy of about 0.3 eV/amu to each particle incident on the sensor collector. Orbital velocities near 5 km s^{-1} at Mars provide an energy a little more than 0.1 eV/amu. In contrast the thermal energy of ions or electrons with a temperature of 1200 K is about 0.1 eV and the equivalent thermal speeds ($\sqrt{2kT/m}$) are about 4.4 km s^{-1} for H+ ions and about 190 km s^{-1} for electrons.

Limitation of the sensor acceptance angle may not always be prudent, or necessary, particularly if the particle thermal speed is much larger than the particle kinetic energy with respect to the sensor, as is the case for thermal electrons. For example a retarding potential analyzer is commonly used to determine the energy distribution of low energy electrons (<100 eV). In this case the detector, described elsewhere in this volume, is called a Langmuir probe in recognition of the pioneering work of Langmuir to the theory of current collection to a conductor in a plasma [*Mott-Smith and Langmuir*, 1926]. Also, when detecting ions, it may not always be sensible to restrict the acceptance angle of the sensor. If the vehicle is spinning, for example, or the direction of the incident ions is highly variable, then a spherical geometry may be preferred. Such a geometry almost always allows incoming ions access to the collector. Then the ion temperature can always be derived, but the lack of directional information means that the direction of the incoming ions is not known. In all cases an expression for the particle flux having access to the collector is determined by integrating the velocity distribution function to include all those particles with velocities allowing access to the collector. For a spherical probe, this gives rise to a somewhat complicated expression [*Medicus*, 1962, *Sagalyn et al.*, 1963] the significance of which is discussed by *Raitt* [1997] in this volume.

Here we will describe a planar RPA used to determine the energy distribution of ambient thermal ions. The term planar refers to the configuration of the grids, which control the energy of the ions that have access to the detector, and to the aperture plane defining the entrance to the detector itself. In its simplest configuration a planar RPA consists of a planar circular entrance aperture followed by a series of planar grids that precede the detector itself. Figure 1 shows a schematic representation of such a sensor where the detector is a solid metal conductor at which the current can be measured by a sensitive electrometer. The arrangement of the entrance aperture and the collector provides a restricted access such that only particles with velocities approximately perpendicular to the entrance aperture have access to the collector. This configuration has grown in sophistication since the early sixties [*Knudsen*, 1964] and has provided important data in the ionospheres of Earth [*Hanson et al.*, 1970], Venus [*Knudsen et al.*, 1980], and Mars [*Hanson et al.*, 1977]. A sensor, such as that shown in Figure 1 is typically employed when the vehicle is three axis stabilized. It will then be mounted to view approximately parallel to the spacecraft velocity vector, the so called ram-direction, and will have an unrestricted view in that direction.

When operating in the ion mode the grid G3 will be biased negatively with respect to the sensor ground. A potential of about -15 V will prevent the access of thermal electrons to the collector and will additionally suppress any photoemission of electrons from the collector surface in the presence of sunlight. The grid G2 usually constitutes a grid pair to which a positive retarding potential is applied. The use of a grid pair provides a planar potential distribution to a high degree of approximation [*Hanson et al.*, 1972] and thus does not change the energy distribution of the incoming ions. For typical spacecraft orbital velocities at zero retarding volts all ions crossing the aperture plane have access to the collector, while at potentials of 30 volts no ions with mass less than 60 amu will have access to the collector. This voltage range then effectively spans the energy range of all major planetary ion species. A grounded shield grid, G4, closest to the collector, in combination with G3, serves to eliminate induced currents to the collector from time varying potentials applied to the retarding grids. The entrance grids G1 are maintained at the sensor ground to ensure that no internally applied potentials influence the energy of the ions outside the sensor.

For a planar sensor, for which the plasma is incident with a kinetic energy that exceeds the thermal energy, the flux of ions that have access to the collector is rather straightforwardly derived by integrating the one dimensional velocity distribution function along the look direction of the sensor and noting that only those ions with

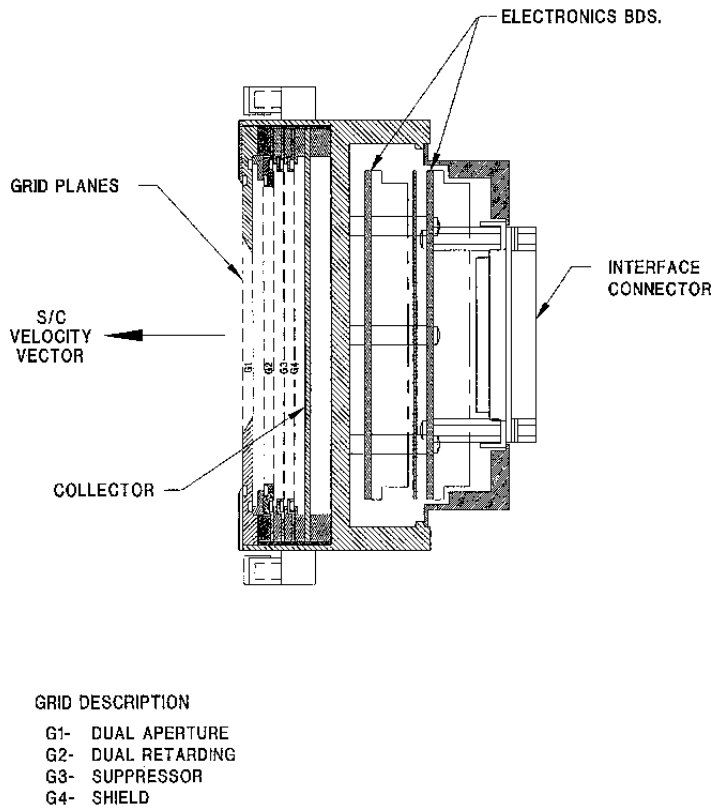

Figure 1. Schematic cross-section of the planar RPA sensor illustrating the arrangement of internal grids required to perform the retarding potential analysis of thermal ions.

energies greater than the potential seen at the retarding grid will reach the collector. Note that the sensor ground may be at some potential ψ_s with respect to the plasma. Thus for a given retarding potential R_v, the potential P seen by the ions will be $R_v + \psi_s$. If the incident kinetic energy of the ions is less than their thermal energy then the sensor acceptance angle and the nature of the sheath potential must also be considered [*Comfort et al.*, 1982]. In the case that the energy distribution of the ions is an isotropic Maxwellian moving supersonically with respect to the sensor then the ion flux is given by [*Whipple*, 1959]

$$\phi_i(P) = \frac{N_i}{2} V_r \left[1 + erf(\beta_i f_i) + \frac{1}{\sqrt{\pi}\beta_i V_r} \exp\left(-\beta_i^2 f_i^2\right) \right] \quad (1)$$

where

$P = q(R_v + \psi_s)$ is the potential of the retarding grid with respect to the plasma,

N_i is the concentration of species i,

V_r is the velocity of ions with respect to the sensor along the sensor look direction,

$\beta_i = \left(m_i / 2kT_i\right)^{1/2}$ is the inverse of the most probable thermal velocity for species i,

$f_i = V_r - \left(2P / m_i\right)^{1/2}$

By stepping through a series of discrete potentials applied to the retarding grid, and recording the ion current, an I-V characteristic is described by the addition of the contributions from constituent ions each given by (1). Figure 2 shows a selection of I-V characteristics obtained from the RPA on Atmosphere Explorer-C [*Hanson and Heelis*, 1975]. The curve in the first panel was taken in the presence of only 0+ and H+ where the H+ concentration exceeds the O+ concentration by a factor of four. Note that if the ions had a temperature of 0K then the curve would describe two step functions occurring at the retarding voltage corresponding to the ram energy of the ions with respect to the sensor. This is illustrated by the dashed lines in panel 1. This ram energy is given by

$$\tfrac{1}{2} m (Vs_r + V_r)^2 - q\psi_s \quad (2)$$

where the ram velocity is composed of the spacecraft velocity along the ram direction Vs_r, and the ambient ion drift velocity along the ram direction V_r. It is usually the case that the spacecraft velocity is much larger than the ambient ion drift velocity and the sensor potential is generally about -0.8V with respect to the plasma. Thus these step functions would occur at about 1.1 and ~~6.1~~ 6.1 volts for H+ and O+ respectively. In practice the step functions are broadened by the effect of a finite temperature as expressed in (1). To first order the thermal width of the I-V curve is given by

$$m_i Vs_r V_{th} \quad (3)$$

where V_{th} is the thermal velocity of the ion species. For O+ ions at 1500 °K this broadening is about 1.6 V when Vs_r is 7.5 km s^{-1}. This broadening is far less than the separation in energy of major species like H+, He+, O+, and molecular ions. However, thermal broadening encompasses the ions O+ and N+ and the molecular species N_2+, NO+, and O_2+. The relative concentration of these species must therefore be specified for optimal analysis.

With appropriate least square fitting to (1) both the ram energy of the ions and the ion temperature can be recovered rather precisely. Examination of (2) indicates that the ram energy for any ion species has a contribution from both the ambient ion drift and the sensor potential. These two parameters cannot be recovered from the retarding potential characteristic containing only one ion species. Thus either an independent measure of sensor potential with respect to

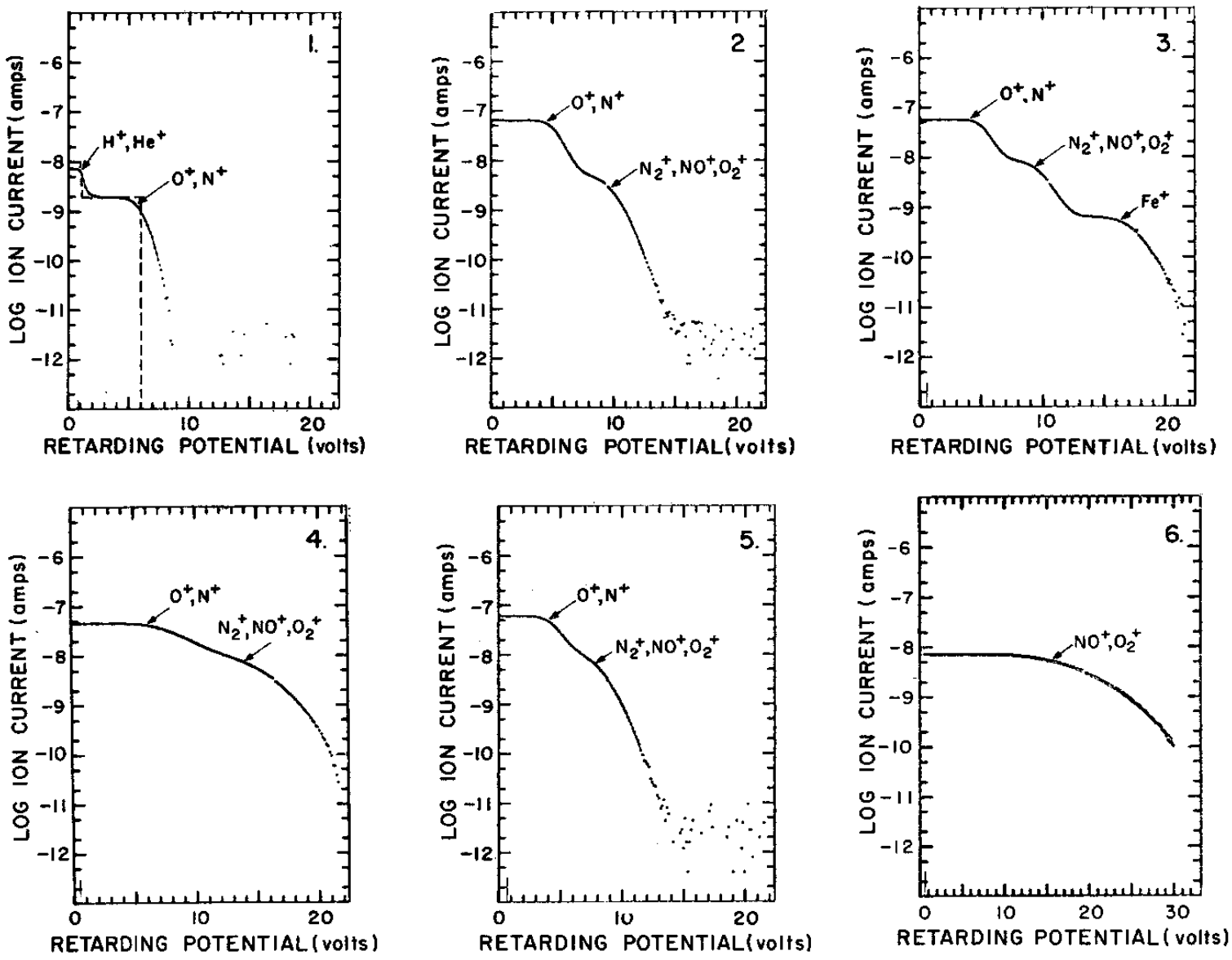

Figure 2. The different I-V characteristics observed in the ionospheric environment of Atmosphere Explorer serve to illustrate the advantages and difficulties in retrieving ionospheric parameters from a planar RPA with a solid conductor collector. See text for details.

the plasma is required, or a retarding potential characteristic for another species, for which the ambient ion drift is the same, is required.

It should be noted that the utilization of a conducting collector for the detector produces a mass-integrated signal. That is, at smaller retarding potentials the ion current for smaller masses is added to that for larger masses. As a practical matter the current for smaller masses cannot be easily separated from that for larger masses if the smaller mass concentration is less than about 5% of the total. In addition, there is a practical limit to the current magnitude that can be detected. For modern electrometers this is about 2×10^{-11} A. Taking account of the fact that the ambient species current must be retarded by about a factor of 3 to produce a meaningful I-V characteristic, and that a typical RPA sensor will have an effective area of about 5 cm^2, this places a lower limit of about 100 cm^{-3} on the ion concentration for which the temperature can be derived using a conducting collector for the detector on a vehicle with orbital velocity 7.5 km s^{-1}. With these limitations the presence of two ion masses can be frequently detected in the ionosphere. Examples are shown in panel 3 of Figure 2 where, the molecular ion species, and meteoric ions Fe+, can all provide easily separated signals subject to the relative concentration arguments mentioned earlier. When two such species are present both the ram drift velocity and the sensor potential can be derived from (2) with the assumption that each species velocity is the same.

However, there are locations, in the middle F-region for example, where only a single ion species can be detected. In this case the sensor potential must be independently specified and can be derived from the electron retarding potential characteristic of a Langmuir probe. However, if the probe is not located at the RPA sensor plane then further manipulation involving geomagnetically induced potentials may be required before the measurements can be utilized in the RPA analysis [*Anderson et al.*, 1994].

Fitting to the measured I-V characteristics requires specification of the ion masses that are present and a subsequent least-squares analysis procedure using the function in (1). When the dominant ion species are well separated in mass this requirement presents no difficulty. For example at the F-region peak and above the dominant ion species are either O+, He+ or H+. A sensor in orbit at F-region altitudes provides these ions with energies of about 5.5 eV, 1.3 eV and 0.3 eV, respectively. They are thus easily resolved in energy subject to the mass-integration difficulties mentioned earlier. In the lower F-region and E-region, the dominant species can be molecular ions with atomic mass units of 28, 30, and 32. As mentioned earlier it is generally difficult to resolve these masses in energy since their energy separation is less than the thermal width of the I-V characteristic. This difficulty is illustrated in panel 6 of Figure 2. With comparable number densities they cannot be treated independently in analyzing an I-V characteristic obtained from a conducting collector. In some cases the derivative of the ion current with respect to the retarding potential may be obtained. The techniques for electronically deriving this signal are described elsewhere in this volume by *Raitt et al.*, [1997]. Some advantages accrue from this technique in that it provides a mass-differentiated signal. However, the use of modern analog to digital converters and fast computers can equalize most of these advantages over using the original I-V characteristic.

The lower limit on the ion concentration, the limits on relative density, and the mass resolution, imposed by the use of a solid conducting collector can be overcome by using a differential mass detector such as an ion mass spectrometer [*Chappell et al.*, 1981]. In this case the limitations are only those placed on the time taken to describe the I-V characteristic, as discussed later.

For a given mass species this characteristic is a unique single valued function and only about 8 points per mass species are required to adequately define the curve for analysis. In practice the location of the 8 points needs to be chosen with some care and generally some on-board processing is employed to select 6 to 8 appropriate points from a larger number (16-24). The larger number of points are taken at discrete retarding voltages that are accessed from look up tables and span the energy range of interest. Dwell times of 8 to 16 ms at each step result in the complete I-V characteristic being completed in 0.25 to 0.5 seconds. Rather more specialized I-V sweeps can be performed at a 10 Hz rate [*Hanson et al.*, 1973] but it should be understood that the requirement to scan a retarding voltage range provides an inherent limit on the time resolution for derivation of the geophysical parameters from an RPA.

PLANAR ION DRIFT METER

An ion drift meter is a device that measures the arrival angle of ions with respect to the sensor look direction. It may be used in conjunction with the planar RPA to obtain the ion drift velocity vector. The IDM is a planar device with a geometry similar to that of the RPA. This geometry was first employed by *Hanson et al.* [1973] although alternative geometry's have been utilized [*Galperin et al*, 1974]. A cross-section of the IDM is shown schematically in Figure 3. The sensor is also mounted to view in the direction parallel to the satellite velocity vector. The sensor relies on the fact that when a satellite is moving supersonically with respect to the plasma, the entrance aperture will produce a collimated ion beam within the sensor. After traversing a field-free region the ion beam is incident on a segmented collector. The grid G6, immediately preceding the collector, is biased negatively with respect to sensor ground. It serves to prevent electrons from accessing the collector and to suppress secondary electron emission from the collector in the presence of sunlight. The grids preceding the suppresser grid and the aperture grids are grounded to provide a field free drift space through which the plasma can move without changing its initial arrival angle. Outside the entrance aperture, which produces the collimated beam are two more grids. The outer most grid is grounded to ensure that internally applied potentials do not influence the ambient plasma. A grid G2, just outside the aperture, may be biased positively with respect to ground in order to select the energy of the incoming ions that have access to the sensor. This grid may be utilized to expel H+ ions that frequently have thermal velocities comparable to the satellite velocity and therefore will not produce a highly collimated beam inside the sensor. This repeller potential is applied before the beam is collimated by the entrance aperture and does not therefore affect the incoming arrival angle of the heavier ion species. Figure 4 indicates how the asymmetry in the current collected on each half of the sensor collector is related to the arrival angle, α, of the plasma with respect to the sensor look direction. The ratio

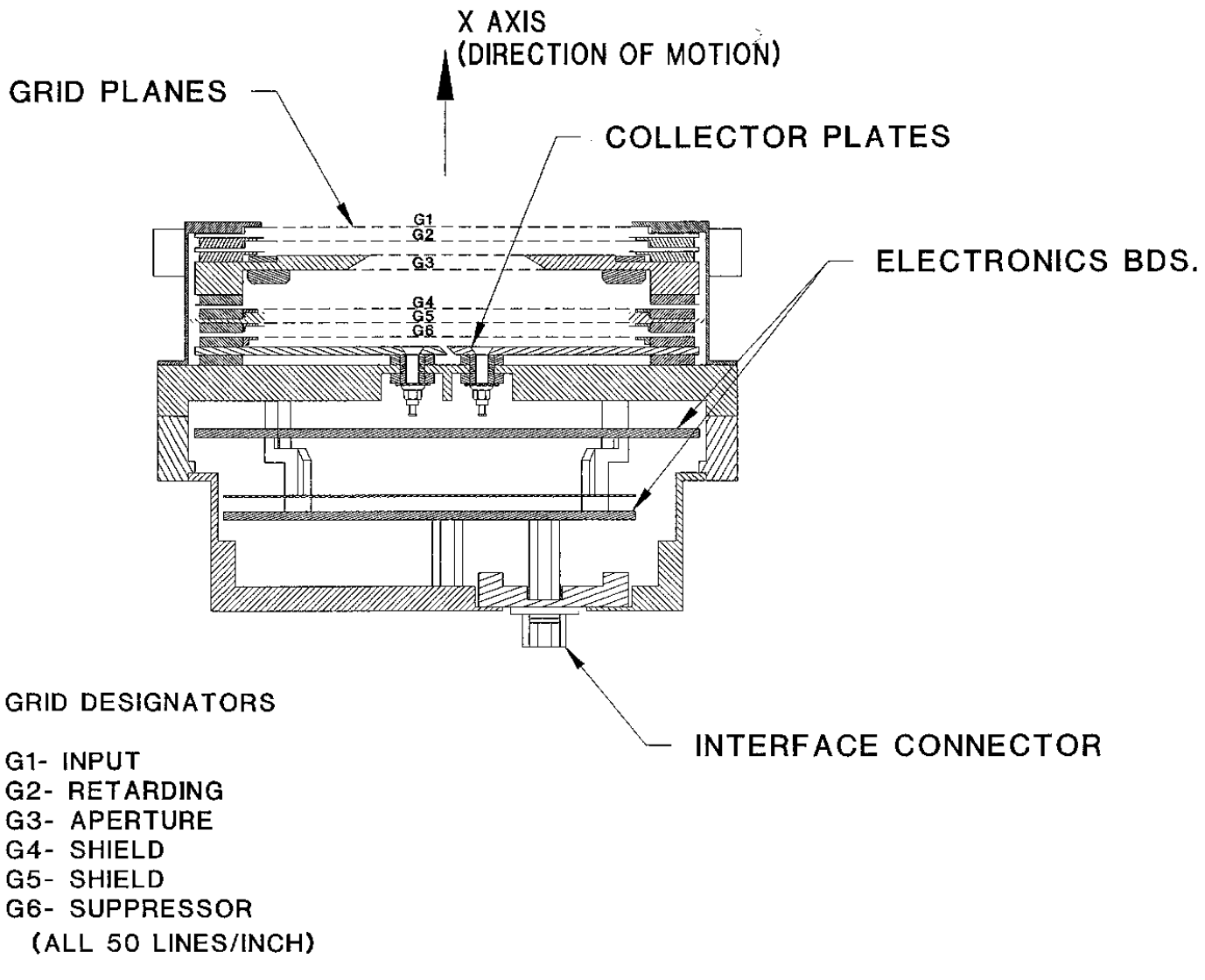

Figure 3. Schematic cross-section of a planar ion drift meter illustrating internal and external grid arrangements and the segmented collector.

of the current to two half-collectors is determined by using two logarithmic electrometers which provide the input to a linear difference amplifier. Then

$$\frac{W - 2D\tan\alpha}{W + 2D\tan\alpha} = \ln I_1 - \ln I_2 = KV_d \qquad (4)$$

where V_d is the difference amplifier output, K is a constant accounting for the sensitivity of the system, and W and D are the square aperture side length, and the effective depth respectively of the sensor.

Figure 5 illustrates how the arrival angle of the plasma, determined by the IDM, is affected by the ram velocity of the ions, determined by the RPA, and the sensor plane potential. Accounting for the acceleration of the ions through the sheath, the transverse drift velocity of the plasma with respect to the sensor in the direction perpendicular to the sensor look direction, and perpendicular to the line separating the collector segments, is given by

$$V_t = \left[\left(Vs_r + V_r\right)^2 - {}^{2q\psi_s}\!/_{m_i}\right]^{1/2} \tan\alpha \qquad (5)$$

Recall that for O+ the satellite orbital velocity provides a ram energy of about 5 eV and the sensor potential with

respect to the plasma is usually less than 1 eV. Inclusion of the increase in the ambient energy of the ions as they are accelerated to the spacecraft potential can change the derived transverse velocity by 1–10% over excluding this effect. The expression in the square bracket is derived directly from the RPA but may also be recovered from the separated parameters if necessary. Thus the transverse velocity perpendicular to the sensor look direction and perpendicular to the line separating the collector halves, is directly determined from the output of the difference amplifier.

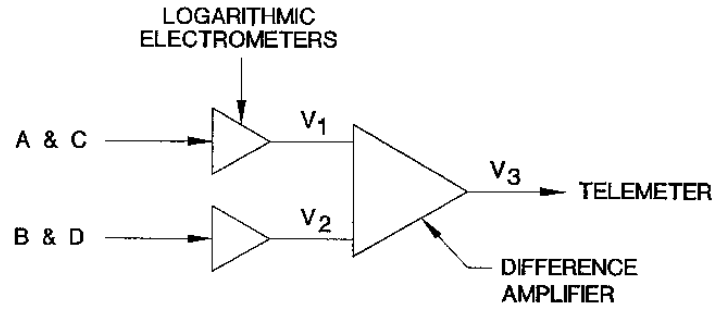

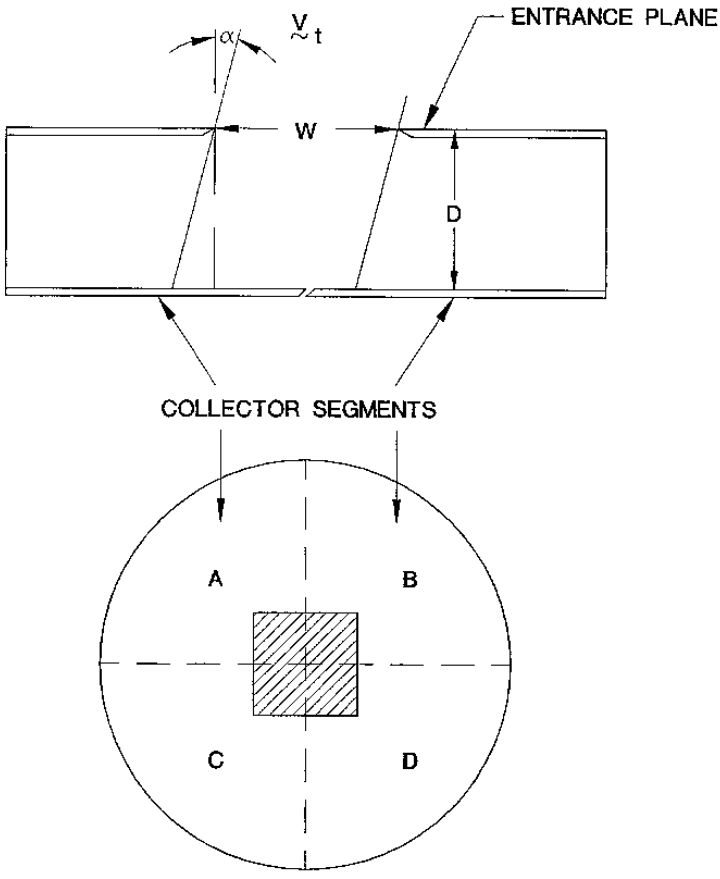

Figure 4. The ion arrival angle is measured by the IDM by determining the asymmetry in the current collected from two halves of a segmented collector.

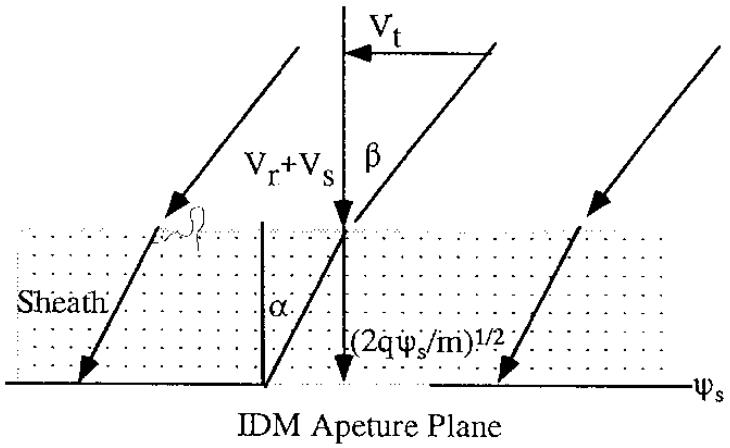

Figure 5. Ambient ions are accelerated through the spacecraft sheath potential and account of this acceleration decrease the apparent ion arrival angle as shown.

Notice that each half-collector is selected by appropriately connecting separate quadrants labeled A, B, C, and D in Figure 4. Connecting A+B and C+D will allow one ion arrival angle to be derived while connecting A+C and B+D will allow another mutually perpendicular arrival angle to be derived. Thus two mutually perpendicular arrival angles can be measured by alternating the connections to the logarithmic electrometers in this manner.

This technique requires careful matching of each of the logarithmic electrometers performance over a range of temperatures, so that offset differences between each one are not interpreted as signal. In practice this may be difficult to accomplish. However, differences in the offsets can be eliminated by the following technique. The original electrometer inputs are inverted and the difference amplifier output established as a zero level. Then the original electrometer inputs are re-established and the difference amplifier output relative to the new zero is proportional only to the ratio of the currents and thus to the ion arrival angle [*Hanson and Heelis*, 1975]. Alternatives to the switching arrangement described here have been utilized to avoid the introduction of switching transients into the system at low ion currents [*Heelis et al.*, 1981]. However, such an arrangement suffers from the inability to remove differences in the electrometer outputs for the same input and is therefore favored only when some significant errors in the absolute value of the drift velocity can be tolerated.

The IDM functions by measuring the ratio of the ion currents on two halves of a segmented collector. The measurement limitations in the device itself are determined by the capabilities of the logarithmic electrometers. Unlike the RPA, the IDM has no time varying potentials and thus arrival angle measurements can be obtained at any sample rate within the frequency response of the

Table 1. Measurement capabilities of a planar RPA and IDM

Geophysical Parameter	Ion Concentration Range	Parameter Range	Accuracy	Sensitivity
Ion Concentration	60 to $6x10^6$ cm^{-3}	10^2 to $6x10^6$ cm^{-3}	±5%	1%
Ion Temperature	10^2 to $6x10^6$ cm^{-3}	300°K to 10000°K	±10%	50 °K
Ram Ion Drift	10^2 to $6x10^6$ cm^{-3}	-6 km s^{-1} to + 6 km s^{-1}	±10%	10 m s^{-1}
Transverse Ion Drift	10^2 to $6x10^6$ cm^{-3}	-5 km s^{-1} to + 5 km s^{-1}	±10 m s^{-1}	1 m s^{-1}

electronics. This is practically limited to between 1 and 2 KHz in ion concentrations above 10^4 cm^{-3} and reduces to 100 Hz in densities below 10^3 cm^{-3}. Within these restrictions the IDM can detect changes in the ion arrival angle as small as 0.01°. Remember that this instrumentation only functions well in the presence of an ion species moving supersonically with respect to the sensor and therefore has poor sensitivity when exposed to H+. In practice the repeller grid is used to exclude H+ from the sensor and the instrument will continue to function well in the presence of heavier ion species with concentrations greater than 100 cm^{-3}.

DRIFT VELOCITY AND ELECTRIC FIELD MEASUREMENTS

Table 1 summarizes the measurement capabilities of a typical RPA/IDM sensor that might be utilized in the upper F-region. It is most important to appreciate that the drift velocity directly measured by the RPA and the IDM is the velocity of the ions with respect to the sensor. Such a sensor will be carefully mounted on a satellite so that the look direction of the sensor, and in turn the mutually perpendicular directions of the arrival angle measurements, can be accurately related to the reference axes of the satellite. The ambient ion drift that is of geophysical interest is determined by removing the contribution of the motion of the satellite from each of the measurements. This requires the inertial attitude of the satellite with respect to the satellite velocity to be accurately known. For a satellite where the velocity is approximately aligned along the sensor look direction, designated by x, the satellite velocity along the look direction is given by

$$V_x = V_s \cos\delta \tag{6}$$

where δ is the angle between the satellite velocity vector V_s, and the look direction. This is a weak function of δ and for small angles the errors imposed by using V_s itself or from errors in specification of δ are quite small. However the calculated velocity along a transverse direction due to an error $\Delta\delta$ is given approximately by

$$\Delta V_t = V_s \sin\Delta\delta \approx V_s\Delta\delta \tag{7}$$

This is quite a strong function of angle and for a satellite velocity of 7.5 km s^{-1} an error of 1° corresponds to an error in the transverse velocity of 140 ms^{-1}. Therefore the uncertainty in determining the transverse ion velocity is significantly determined by the accuracy with which the inertial attitude of the vehicle can be derived.

COMPARISON OF ELECTRIC FIELD AND ION DRIFT MEASUREMENTS

It should be understood at the outset that measurement of the ion drift velocity vector and the electric field vector are not equivalent functions. However in regions where the ion velocity perpendicular to the magnetic field is dominated by the electric force and $\mathbf{V}_\perp = \mathbf{ExB}/B^2$, then a measurement of the electric field vector and the ambient magnetic field vector can be used to determine the ion drift velocity perpendicular to the magnetic field. This method is different from a measurement of the complete ion drift velocity vector since significant diffusive motion of the ions can take place along the magnetic field that is not exposed by a measurement of **E**. Similarly a measurement of the ion drift velocity vector and the ambient magnetic field will not expose the existence of electric fields parallel to the magnetic field. This may not be a significant deficiency in the F-region but nevertheless the difference between these measurements should be appreciated. The difference is even more important when the relationship $\mathbf{V}_\perp = \mathbf{ExB}/B^2$ does not hold. At altitudes below 200 km, for example, significant departures between the perpendicular components of the ion drift and the electric field may exist and in fact some key scientific issues may center around understanding the nature of the differences

between these quantities. In regions when a comparison can be sensibly made then the relative strengths and weaknesses of each technique are extensively discussed by *Hanson et al.*, [1993].

Knowledge of the inertial attitude of the sensor is also a large factor determining the accuracy with which ambient electric fields can be determined. Just as the measurements from plasma sensors require subtraction of the satellite velocity in the satellite reference frame, derivation of the electric field also requires this information for subtraction of the $\mathbf{V}_s\mathbf{xB}$ induced electric field. When comparing the measurements, the errors in inertial attitude determination that apply to these tasks, cancel. However, the conversion of **E** to **V**, or **V** to **E**, for comparison, require specification of the magnetic field vector in the spacecraft reference frame. If the magnetic field vector is specified using a global reference model [*Langel and Estes*, 1985] then errors in specification of the inertial attitude of the spacecraft reappear in the comparison.

At low latitudes the use of a global magnetic field model is extremely accurate and the problems reduce to the clarity with which very small electric fields and ion drifts can be detected. The IDM is an extremely sensitive device and when the ion drift component of interest is a transverse component measured by this device then the accuracy is almost solely determined by the accuracy of the vehicle attitude determination system. In the case that the RPA is significantly involved in the velocity determination then the uncertainties in measurements derived by E-field detectors and plasma sensors are comparable and under normal conditions are of the order of 10 ms^{-1}. At high latitudes the drift velocities and electric fields are larger than those at lower latitudes, and knowledge of the magnetic field vector is required to provide a common quantity for comparison. The magnetic field may also deviate from model values due to field-aligned currents. Figure 6 taken from the work of *Hanson et al.*, [1993] serves to illustrate the major points to consider. Here the velocity vector measured by the RPA and IDM on DE-2 has been translated to an equivalent electric field for comparison with the Vector Electric Field Instrument measurements of the same parameter. Note that the comparison is very good and even at relatively small scales it is difficult to see the differences between both measurements plotted in panels b) and c). The differences shown in panels d) and e) illustrate the measurement problems faced by each technique. First it should be noted that they are very small, in most cases being less than 2 mVm^{-1}. The waviness in panel e) is caused by oscillations of the electric field boom, and more careful consideration of contact potential could probably remove the larger scale variations seen here. However, the variations at the smallest scale sizes occur in the presence of very large energetic particle fluxes. Such fluxes could produce asymmetries in the current observed by the IDM that are erroneously interpreted as ion drifts. These particles may also produce small scale changes in the vehicle potential that affect the measurements from the IDM. If they also produce spatial variations in the ion concentration with spatial scale sizes comparable to the electric field probe separation distance, then they may influence these measurements. Finally the presence of field aligned currents may effect changes in the magnetic field vector that are introduced as errors in attempting to translate ion drift measurements to electric fields.

INSTRUMENT ACCOMMODATIONS

It should be apparent that the RPA and IDM sensors are sensitive to very small changes in the thermal energy and the kinetic energy of the ion species. It is therefore important to assure that the sensor, and the satellite to which the sensor is mounted, do not produce large changes in these energy distributions. Note that potentials applied within the sensors are referenced to a chassis ground. This ground must be maintained within reasonable limits (±5V) of the plasma potential if reasonable retarding potentials are to be utilized and the thermal energy distribution is to be uncontaminated. If this reference ground is the satellite ground then the satellite potential itself must be maintained close to the plasma potential. Due to the large difference in the thermal speeds of electrons and ions, the spacecraft will generally attain a small negative potential with respect to the plasma in order to equalize the ambient ion and electron currents. However, any positively biased potentials will attempt to collect thermal electrons, and will result in a bias of the spacecraft ground negatively with respect to the plasma, in order to prevent this collection. A large negative potential with respect to the plasma may provide the incoming ions with energies in excess of those that can be retarded by internally applied potentials. It is prudent therefore to ensure that positively applied potentials are not exposed to the plasma. The largest concern in this area is in the construction of a solar power array, which may have multiple interconnects that are not insulated from the plasma. In such circumstance it is necessary to consider methodologies by which the plasma sensors can be electrically isolated from the spacecraft [*Zuccaro and Holt*, 1982].

Even when the spacecraft potential is carefully controlled it is wise to provide a planar conducting area around the plasma sensor apertures to ensure that the electric fields experienced by the plasma are normal to the aperture plane. Such a large plane conducting surface facing in the ram

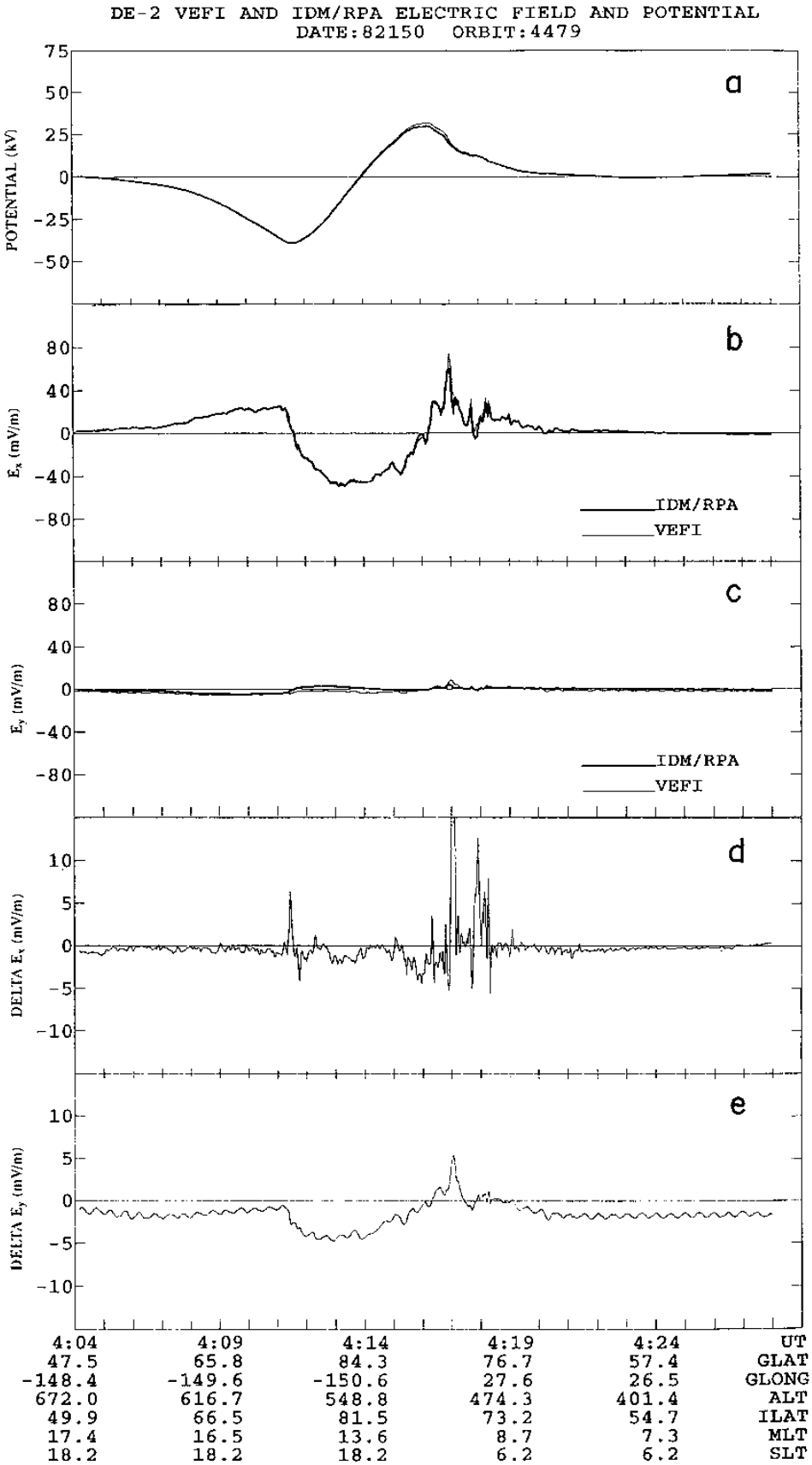

Figure 6. A comparison of the directly measured electric field and that derived from the ion drift velocity measured on the DE-2 spacecraft. Differences between the two measurements are very small but serve to highlight some of the difficulties encountered by each technique. [After *Hanson et al.*, 1985]

direction may be the only surface from which thermal ions can be effectively collected. Thus this surface will also serve as a source of ambient ion current that will assist in neutralizing the ambient electron current that can be collected from any exposed conductor on the spacecraft.

SUMMARY

The use of planar sensors for measurement of the temperature and drift of thermal plasma has been successfully utilized in many instances when the local plasma concentration is greater than 100 cm^{-3}. In such circumstances the use of a solid conducting collector from which the ambient plasma current can be detected is quite satisfactory. However, the relative composition of charged particle species in planetary ionospheres frequently dictates the need for mass resolved retarding potential characteristics. These are obtained by using a mass analyzer detector, that additionally provides the capability to observe much lower species concentrations. When the instruments are mounted on a vehicle allowing a view of the plasma along the satellite velocity vector, the resulting ion flux versus retarding potential allows derivation of the kinetic energy and the temperature of the ion species. Modern electronics and ground-based computational procedures allow derivation of plasma temperatures and velocities with high quality. While the IDM has the capability to sample ion arrival angles at very high frequencies (1-2 KHz), a single RPA sensor has a time resolution for geophysical measurement that is limited by the requirement to adequately describe the energy distribution of the ion species. Present instruments can provide good data with a temporal resolution of 0.25 secs. The increasing use of instrument intelligence and multiple sensors may dramatically increase this resolution in the future.

Acknowlegements. This work is supported by NASA grant NAGW 4429 to the University of Texas at Dallas.

REFERENCES

Anderson, P. C., W. B. Hanson, W. R. Coley and W. R. Hoegy, Spacecraft potential effects on the Dynamics Explorer 2 satellite, *J. Geophys. Res.*, 99, 3985-3997, 1994.

Chappell, C. R., S. A. Fields, C. R. Baugher, J. H. Hoffman, W. B. Hanson, W. W. Wright, H. D. Hammack, G. R. Carignan and A. F. Nagy, The retarding ion mass spectrometer on Dynamics Explorer-A, *Space Sci. Instrum.*, 5, 477-491, 1981.

Comfort, R. H., C. R. Baugher and C. R. Chappell, Use of the thin sheath approximation for obtaining ion temperatures from the ISEE 1 limited aperture RPA, *J. Geophys. Res., 87*, 5109-5123, 1982.

Galperin, Y. I., V. N. Ponomarev and A. G. Zosimova, Plasma convection in the polar ionosphere, *Ann. Geophys., 30*, 1-7, 1974.

Hanson, W. B., W. R. Coley, R. A. Heelis, N. C. Maynard and T. L. Aggson, A comparison of in-situ measurements of E and -VxB from Dynamics Explorer 2., *J. Geophys. Res., 98*, 21,501-21,516, 1993.

Hanson, W. B., S. Sanatani and D. Zuccaro, The Martian ionosphere as observed by the Viking retarding potential analyzers., *J. Geophys. Res., 82*, 4351-4363, 1977.

Hanson, W. B. and R. A. Heelis, Techniques for measuring bulk gas-motions from satellites, *Space Sci. Instrum., 1*, 493-524, 1975.

Hanson, W. B., D. R. Zucarro, C. R. Lippincott and S. Sanatani, The retarding potential analyzer on Atmosphere Explorer-C, *Radio Sci., 8*, 333, 1973.

Hanson, W. B., D. R. Frame and J. E. Midgley, Errors in retarding potential analyzers caused by nonuniformity in the grid-plane potential., *J. Geophys. Res., 77*, 1914-1922, 1972.

Hanson, W. B., S. Sanatani, D. Zuccaro and T. W. Flowerday, Plasma measurements with the retarding potential analyzer on Ogo 6, *J. Geophys. Res., 75*, 5483-5501, 1970.

Heelis, R. A., W. B. Hanson, C. R. Lippincott, D. R. Zuccaro, L. L. Harmon, B. J. Holt, J. E. Doherty and R. A. Power, The ion drift meter for Dynamics Explorer-B, *Space Sci. Instrum., 5*, 511, 1981.

Knudsen, W. C., Evaluation and demonstration of the use of retarding potential analyzers for measuring several ionospheric quantities., *J. Geophys. Res., 71*, 4669-4678, 1964.

Knudsen, W. C., K. Spenner, J. Bakke and V. Novak, Pioneer Venus orbiter planar retarding potential analyzer plasma experiment., *IEEE Trans. Geos. Rem. Sens., 1*, 49-54, 1980.

Langel, R. A. and R. H. Estes, The near-Earth magnetic field at 1980 determined from Magsat data, *J. Geophys. Res., 90*, 2495-2504, 1985.

Medicus, G., Theory of electron collection of spherical probes, *J. App. Phys., 32*, 2512-2520, 1961.

Mott-Smith, H. M. and I. Langmuir, The theory of collectors in gaseous discharges, *Phys. Rev., 28*, 727-763, 1926.

Sagalyn, R., M. Smiddy and J. Wisnia, Measurement and interpretation of ion density distributions in the daytime F region, *J. Geophys. Res., 68*, 198-212, 1963.

Whipple, E. C., The ion trap results in "Exploration of the upper atmosphere with the help of the third soviet sputnik., *Proc. IRE, 47*, 2023-2024, 1959.

Zuccaro, D. R. and B. J. Holt, A technique for establishing a reference potential on satellites in planetary ionospheres, *J. Geophys. Res., 87*, 8327-8329, 1982.

R. A. Heelis, William B. Hanson Center for Space Sciences, Physics Program, University of Texas at Dallas, MS/FO22, Richardson, TX 75083-0688.